Quantum-Chemical Interpretation of Current-Induced Forces on Adatoms on Carbon Nanotubes

Yvan Girard,* Takahiro Yamamoto, and Kazuyuki Watanabe

Department of Physics, Tokyo University of Science, 1-3 Kagurazaka, Shinjuku-ku, Tokyo 162-8601, Japan, and CREST, Japan Science and Technology Agency, 4-1-8 Honcho Kawaguchi, Saitama 332-0012, Japan

Received: April 11, 2007; In Final Form: June 26, 2007

The forces induced by a steady electric current on several atoms, namely, B, C, N, O, and F, adsorbed on a metallic (5,5) carbon nanotube are calculated using the nonequilibrium Green's function technique combined with density functional theory. Atoms are optimized in bridge positions and are found to be either repelled from the tube (C, N, O, and F) or attracted to it (B). The current-induced forces pull the atoms either in the direction of the electron flow (N, O, and F) or in the opposite direction (B and C). These results can be understood in terms of charge transfer, modification of the electron density, and the chemical bonding properties of the scattering states.

1. Introduction

Since their discovery in 1991,[1] carbon nanotubes have been the subject of intense research. New applications of single-walled, multiwalled, doped, filled, functionalized, and diversely modified tubes are developed on a regular basis.[2] Each new idea is more promising than the other and quickly yields numerous publications. The controlled transport of various elements by a nanotube is an interesting possibility for the development of nanotechnologies. We already know that nanotubes can be used as atomic force microscopy (AFM) tips to manipulate various nanostructures[3] but could they not also be used to carry matter directly "on-site"?

Different ways of performing that task have been explored. For instance, a flow of polar molecules *inside* a tube can drag other molecules weakly bonded on the *outside*.[4] A more straightforward idea is to use the carbon nanotube's (CNT's) ability to conduct electricity and expect current-induced forces (or electromigration).[5] As a matter of fact, this possibility has already been tested experimentally and promising results have been obtained for indium[6] or iron[7] nanocrystals "moved" along carbon nanotubes by a variable bias voltage.

From a theoretical point of view, the fundamental nature of the current-induced forces needs to be understood. Di Ventra and co-workers discussed the origin of the forces and whether they can be estimated practically with steady-state calculations (see refs 8 and 9 and references therein). Brandbyge et al.[10] described how a small gold chain would be distorted by an applied current, while Mingo et al.[11] and Heinze et al.[12] investigated the forces experienced by ions in the vicinity of conducting nanotubes. These studies focused on how the current modifies the bonding strength between the atoms. The experiments involving indium have also been investigated through ab initio calculations,[13] showing that a charge-transfer leaves the metal positively charged and induces its diffusion toward the cathode (in the opposite direction to the electron flow).

The present study deals with some of the forces induced by an electric current on single atoms adsorbed on a clean metallic (5,5) single-walled carbon nanotube (SWCNT). Five different adatoms, namely, boron (B), carbon (C), nitrogen (N), oxygen (O), and fluorine (F), are tested. The Keldysh nonequilibrium Green's function (NEGF) formalism combined with the density functional theory (DFT) for electron transport is used to determine the electronic structure of the system under various bias voltages. The forces acting on the adatoms are found to depend on the bias magnitude, the current direction, and the atomic species: they drive the atom away from the tube in the case of O, N, C, and F but attract B toward the tube. They push the O, F, and N atoms slightly in the direction of the electron flow but pull the B and C atoms in the opposite direction. We elucidate the mechanism of these forces using quantum-chemical considerations based on atom's charges, modifications of the electron density, and the bonding nature between the adatoms and the tube's surface. At this level of theory, the inelastic interactions (when vibrationnal modes of the adsorbate are excited by the flowing electrons) have not been taken into account. Depending on the adatom mass and on the current applied, these interactions will generate a local heating and probably facilitate the desorption of the adatoms but this contribution is difficult to quantify.[11] However, the current-

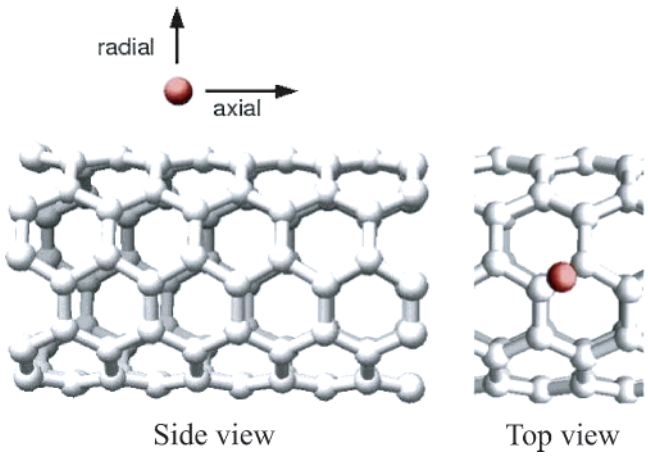

Figure 1. Schematic view of the adsorption site of an atom on a carbon nanotube and definition of the directions.

* Corresponding author.

10.1021/jp0728149 CCC: $37.00
Published on Web 08/01/2007

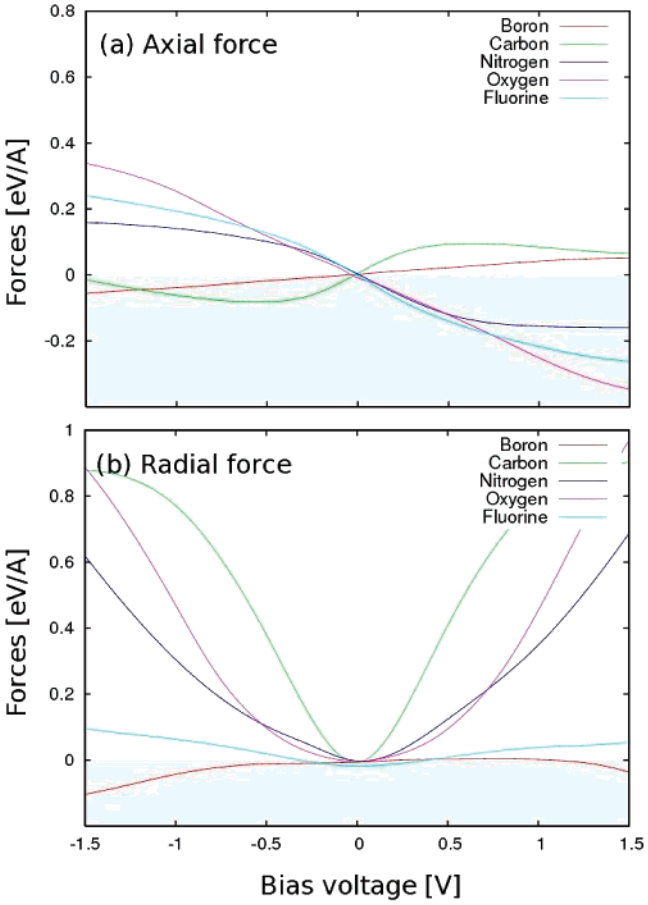

Figure 2. Axial and radial components of forces acting on adatoms depending on the bias voltage. Under a positive bias voltage, electrons flow from the right lead to the left lead. A positive radial force pushes the adatom away from the tube, and a positive axial force pushes it from left to right.

TABLE 1: Mulliken Charges and Atom/Tube Distances

	charge SZ (SZ+P)	distance
B	+0.44 (+0.34)	2.18 Å
C	+0.20 (+0.12)	1.83 Å
N	−0.0 (−0.07)	1.70 Å
O	−0.10 (−0.15)	1.67 Å
F	−0.10 (−0.12)	1.87 Å

induced forces will probably be the most important at the low biases considered, as it is the case in atomic wires.[9]

The paper is organized as follows. Section 2 briefly describes the theoretical tools used in our study. In section 3, we present the results of the calculated forces and our quantum-chemical interpretation. We summarize our findings in section 4.

2. Theoretical Methods

We investigate the current-carrying states of carbon nanotubes and determine the force acting on adatoms by the NEGF+DFT technique, which has been widely used in the past five or six years. We use the commercially available Atomistix Tool Kit (ATK).[14] This code is the natural evolution and extension of the TranSIESTA-C,[15] and uses numerical atomic orbitals and norm-conserving pseudopotentials. The method's premise is to divide the system into three regions: (i) the left and (ii) right electrodes and (iii) the scattering region in between. The Green's function of the scattering region includes the self-energy generated by the leads through a self-consistent scheme. Transmission functions, density of states, and current−voltage

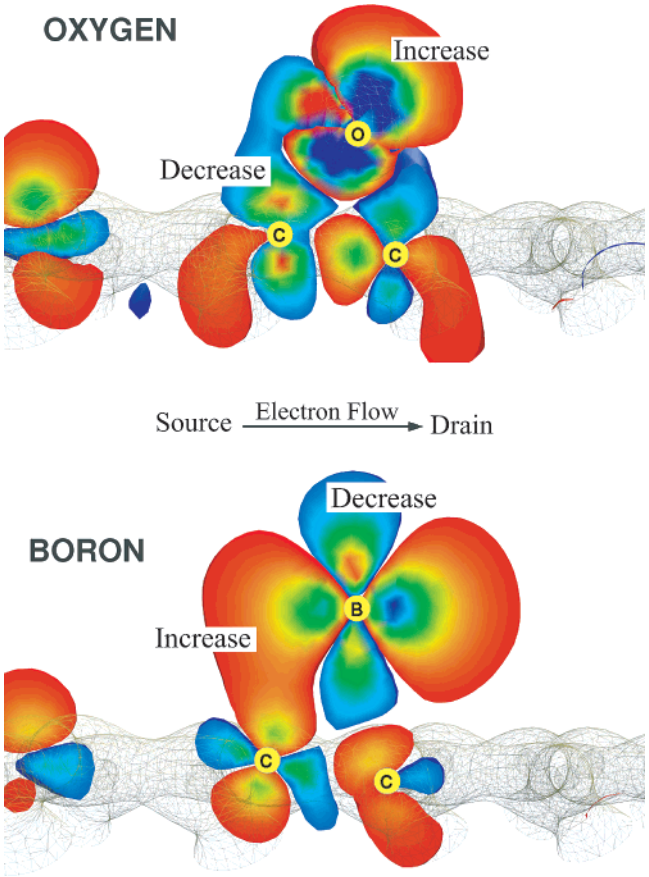

Figure 3. Difference in electron density due to the bias voltage for oxygen and boron in the C−O−C and C−B−C planes. Red and blue zones show an increase and decrease in electron density due to the bias voltage, respectively.

characteristics of two-probe systems are then available (see ref 15 for detailed explanations).

As the NEGF+DFT technique generates a Kohn−Sham Hamiltonian $\hat{H}$ and an associated density matrix $\hat{D}$, the force experienced by the ith atom, F_i, is readily given by the Hellmann−Feynman theorem:

$$F_i = Tr[\hat{F}_i \hat{D}] \quad \text{with} \quad \hat{F}_i = -\frac{\partial \hat{H}}{\partial R_i}$$

where $\hat{F}_i$ is the force operator with respect to the ith atom. Our discussion relies mainly on a technique in which only the subset of the Hamiltonian that is associated with the scattering region is diagonalized (once the self-consistent process is over). The eigenstates of this truncated Hamiltonian can be seen as approximated molecular orbitals, localized on the scattering region, but modified by the left and right leads. The real scattering states are related to these eigenstates but broadened and shifted in energy by the interaction with the electrodes. The truncated Hamiltonian is called the molecular projected self-consistent Hamiltonian (MPSH), and we refer to these states as the MPSH states.[16]

3. Results and Discussion

The calculations were performed with five different atoms, namely, B, C, N, O, and F, adsorbed onto a (5,5) metallic carbon nanotube. We used single-ζ basis sets[17] with an local-density approximation (LDA) functional and considered a fairly large scattering region containing 100 carbon atoms (5 unit cells). The left and right leads are semi-infinite nanotubes as well, and

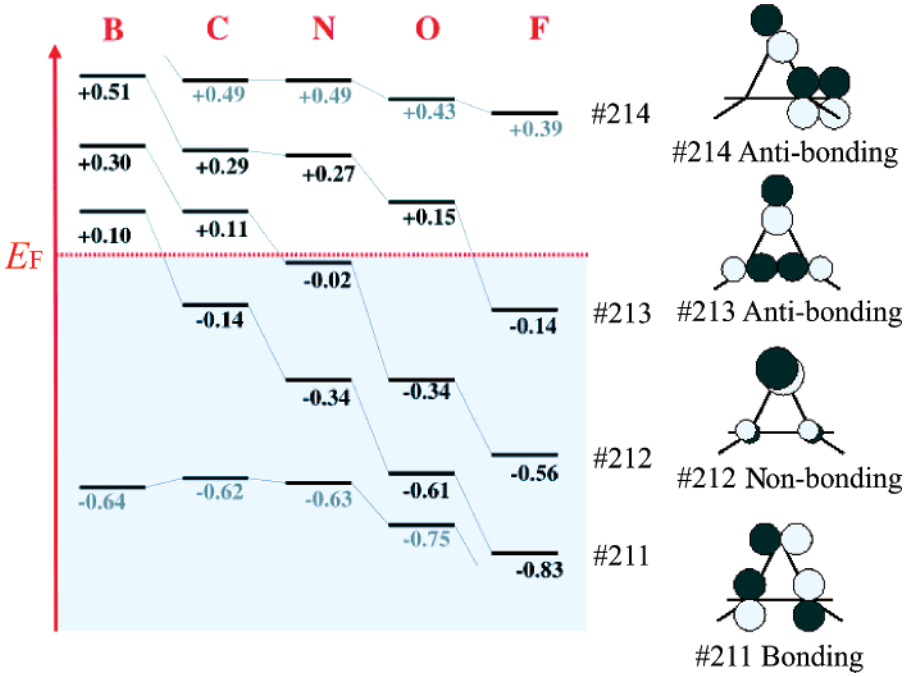

Figure 4. Schematic representation and energies of the MPSH levels near the Fermi energy for B, C, N, O, and F.

their self-energies are obtained from separate bulk calculations under periodic boundary conditions.

The geometries were optimized at zero bias voltage with the atoms in the bridge position, as shown in Figure 1. Adatoms were always found to be equidistant to the two nearest carbon atoms. The distances are given in Table 1. The charge transfers between the adatoms and the tube were estimated by Mulliken population analysis. These estimates are also tabulated in the Table 1. We checked that our scattering region is long enough so that the charge transfer will not affect the boundary regions.

We limited our study to rather low bias voltages (e.g., <1.5 V) to obtain reliable results, although more interesting effects are expected to occur with stronger currents (evaporation or diffusion of adatoms). As a convention, a positive bias voltage implies that the left lead has a lower chemical potential than the right lead (current is from left to right; the electrons flow from right to left). A positive force is defined as being directed toward the right.

The forces exerted on the adatoms under the bias voltage are plotted in Figure 2a,b. The upper and lower panels show the projections of the forces depending on the bias voltage along two directions, axial and radial, respectively (as shown in Figure 1). The forces in the third direction (lateral) are always negligible.

Axial Force. (Figure 2a) The axial forces are rather weak for all five atoms compared with the radial forces in Figure 2b. Three atoms (O, F, and N) are pushed in the direction of electron flow, while the other two (B and C) feel the opposite effect. They are pulled in the direction opposite to the electron flow. There is a loose correlation between the atomic charge of the adatoms and the direction and strength of the forces (see Table 1): B and C are positively charged ($+0.44$ e and $+0.20$ e, respectively) and are pulled against the electron flow (see the axial force in Figure 2a), while F and O are negative (-0.10 e for both atoms), and the forces acting on them are in the direction of the electron flow. Previous calculations involving the indium atom, which is positively charged,[13] gave similar results. Consequently, the qualitative features of the forces on adatoms, except those on the N atom, can be understood in terms of the electrostatic interaction between the charged adatoms and the potential gradient due to the bias voltage. However, the nonlinear behavior of axial forces in the high bias region beyond $|V_{bias}| \sim 0.5$ V remains unclear. A further investigation beyond Mulliken charge analysis is neverthless required. Note that calculations of the charges using polarized basis sets[17] were also done on the same geometries, and they give similar results (see Table 1).

Radial Force. (Figure 2b) The radial force drives the atom away from the tube in the cases of O, N, C and, to a lesser extent, in the case of F. By contrast, B is slightly attracted to the tube. In the case of O, our results were consistent with previous calculations[11] although we obtained higher force values.

The Mulliken charge is key in understanding the axial force but irrelevant to the character of the radial force. Indeed, a good way to understand the origin of the force intuitively is to see how the charge density is self-consistently modified by the bias voltage. Figure 3 illustrates how the electron density changes when a small bias voltage is applied (-1 V), with respect to the zero-bias case, for O and B. The red area is the region of electron density surplus, while the blue area is the region of electron density deficit. The figures display slices of the volumes in the C−O−C and C−B−C planes (i.e., the adatoms and the two nearest carbon atoms) and elucidate why the forces are induced in different directions. For the O case, the current displaces electrons from the C−O bonding zone to an area away from the tube. Thus, the C−O bonds are weakened, and the atom is pulled away from the tube. In the B case, the electron density is slightly increased between the adatom and the tube, and therefore, the radial force becomes attractive. It can also be seen from Figure 3 that the radial force is an even function of applied voltage.

It is possible to go further and rationalize the problem by considering the nature of the scattering states localized on the adatoms. As mentioned in section 2, the shapes and relative energies of the states can be estimated through the MPSH scheme. We calculated the MPSH eigenvalues in the zero-bias case, and those close to the Fermi level are given in Figure 4. We assign numbers to the levels according to their energies:

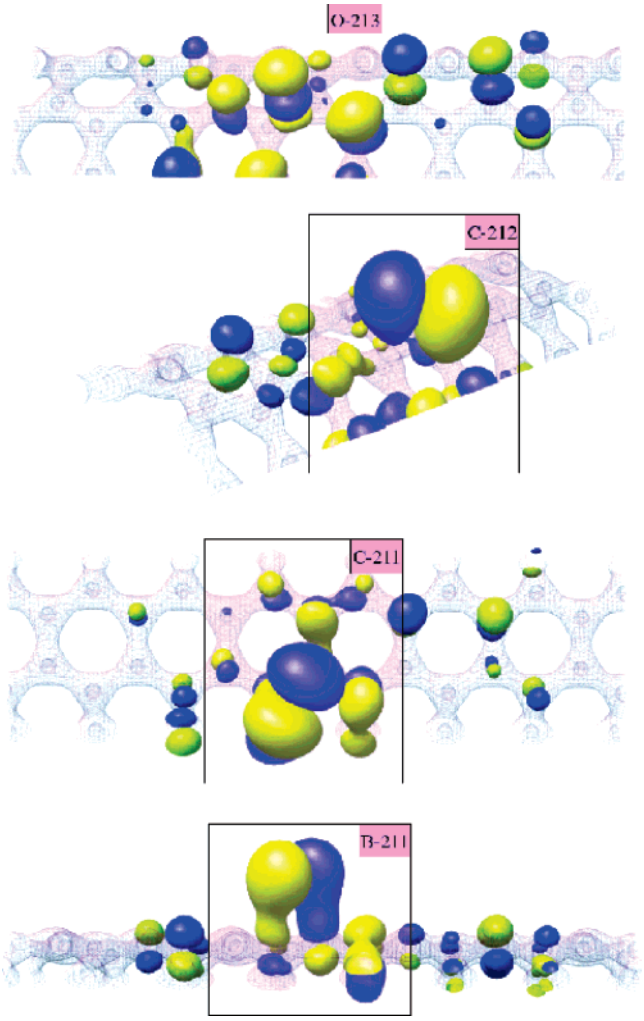

Figure 5. Several selected MPSH orbitals. Colors correspond to the different phases of the states, and the boxes are a visual aid, centered on the adatom.

#1 has the lowest energy; the levels depicted, from #211 to #214, are those surrounding the Fermi level. We observe that the MPSH levels with similar numbers all have similar bonding character, as schematized in Figure 4. As shown on the right-hand side of Figure 4, orbitals #211 have a bonding character between the adatom and the nearest carbon atoms, orbitals #212 are nonbonding, and #213 and #214 have an antibonding character. Several "real" MPSH eigenstates are displayed in Figure 5 to support our statement.

On the basis of the energy diagram in Figure 4, we can make the following assumption, illustrated in Figure 6: When the bias is applied, the scattering electrons from the lead with the higher chemical potential (source) populates the states above the original Fermi level. In a similar way, the state below the Fermi level is depopulated by the electron flow toward the lead with the lower chemical potential (drain). The applied bias voltages have only a small influence on the positions, and the shapes of the MPSH levels discussed here and their energies relative to the middle of the bias windows remain unchanged, as they are in the Figure 4.

In the case of the C atom, according to the diagram (Figure 4), the applied bias should populate level #212 and depopulate level #211. In Figure 7, which shows the variation in electron density under a 1 V bias, we do observe a good correspondence between the populated and depopulated areas and the MPSH orbitals: the # C211 bonding level is depopulated (blue lobes

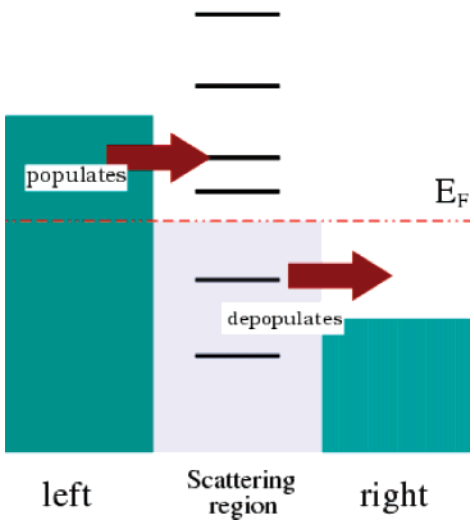

Figure 6. Schematic model for the filling of scattering states. The red line shows the Fermi level at zero bias.

in Figure 7) and the # 212 nonbonding level is populated (red lobes in Figure 7).

The agreement between the level population/depopulations and the density change has been verified for all five calculations: In each case, the level immediately below the Fermi level matches the depopulated regions, and the level immediately above the Fermi level matches the populated region, supporting our interpretation. Remarkably, the distribution of the charge density remains unchanged when the direction of the current is reversed. This is also consistent with the level population/depopulation scheme.

Thus, we conclude that the radial forces of all atoms in Figure 2b can be explained by the energy diagram in Figure 4 as follows:

(1) The C atom is repelled from the tube wall under bias voltage. This stems from the bond weakening due to the populated nonbonding level (#212) and the depopulated bonding level (#211).

(2) The O atom is repelled for a similar reason since the antibonding level (#213) is populated.

(3) The N atom is also repelled because the antibonding level (#213) is populated and the bonding level (#211) becomes depopulated. The nonbonding level (#212) just below the Fermi level does not contribute to the force because this level is neither populated nor depopulated.

(4) The force exerted on the F atom becomes very small because both the depopulated level (#213 below the Fermi level) and the populated level (#214 above the Fermi level) are antibonding.

(5) Only the B atom is attracted to the tube wall by the bonding level (#211 populated).

4. Summary and Outlook

We investigated the forces that are due to the self-consistent redistribution of the electron density exerted on the first-row atoms (B, C, N, O, F) in the periodic table adsorbed on the outer wall of a (5,5) metallic carbon nanotube under bias voltages. We found that the properties of bias-dependent axial and radial components of the force are intrinsically different from each other. The character of axial force is essentially determined by the electrostatic interaction between the induced charge of adatoms and the electrostatic potential induced by

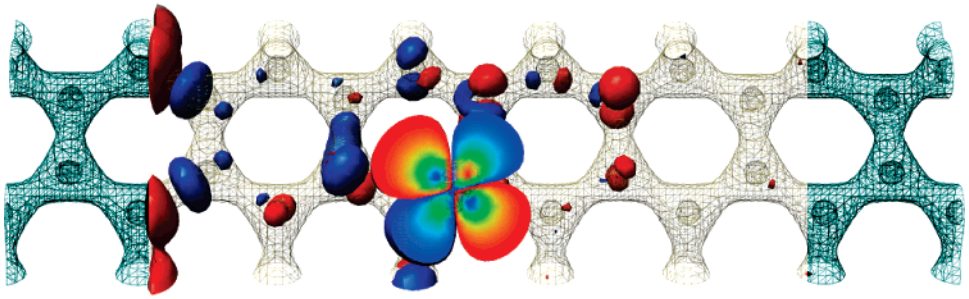

Figure 7. Difference in the electron density under bias voltage. Red and blue zones show the increase and decrease in electron density due to the bias voltage, respectively. The blue lobes match level #C211 and the red lobes match level #C212 (see text and Figure 5).

the bias voltage. In marked contrast, the bias-dependent radial force originates from the modification of electronic scattering states. As a result, the nature of the chemical bonds and the energy-level scheme under a bias voltage sheds light on the properties of the radial forces on all the elements studied. Unresolved problems, that is, an unusual feature of the axial force on a C adatom and possibility of current-induced evaporation and diffusion of adatoms at higher bias-voltages, are important issues from the standpoint of applications and will be the subject of future research. The analysis of forces on semiconducting carbon nanotubes is currently under progress.

Acknowledgment. T.Y. and K.W. acknowledge support from the "Academic Frontier" Project of the Ministry of Education, Culture, Sports, Science and Technology of Japan. Some of the numerical calculations were performed on the Hitachi SR11000s at ISSP, the University of Tokyo.

References and Notes

(1) Iijima, S. *Nature* **1991**, *354*, 56.
(2) Baughman, R. H.; Zakhidov, A. A.; de Heer, W. A. *Science* **2002**, *297*, 787.
(3) Chen, L.; Cheung, C. L.; Ashby, P. D.; Lieber, C. M. *Nano Lett.* **2004**, *4*, 1725.
(4) Wang, B.; Kral, P. *J. Am. Chem. Soc.* **2006**, *128*, 15984.
(5) Kral, P.; Tomanek, D. *Phys. Rev. Lett.* **1999**, *82*, 5373.
(6) Regan, B. C.; Aloni, S.; Ritchie, R. O.; Dahmen, U.; Zettl, A. *Nature* **2004**, *428*, 924.
(7) Svensson, K.; Olin, H.; Olsson, E. *Phys. Rev. Lett.* **2004**, *93*, 145901.
(8) Di Ventra, M.; Chen, Y. C.; Todorov, T. N. *Phys. Rev. Lett.* **2004**, *92*, 176803.
(9) Yang, Z.; Chshiev, M.; Zwolak, M.; Chen, Y. C.; Di Ventra, M. *Phys. Rev. B* **2005**, *71*, 041402(R).
(10) Brandbyge, M.; Stokbro, K.; Taylor, J.; Mozos, J. L.; Ordejon, P. *Phys. Rev. B* **2003**, *67*, 193104.
(11) Mingo, N.; Yang, L.; Han, J. *J. Phys. Chem. B* **2001**, *105*, 11142.
(12) Heinze, S.; Wang, N. P; Tersoff, J. *Phys. Rev. Lett.* **2005**, *95*, 186802.
(13) Ribeiro, F. J.; Neaton, J. B.; Louie, S. G.; Cohen, M. L. *Phys. Rev. B* **2005**, *72*, 075302.
(14) Atomistix Home Page. http://www.atomistix.com.
(15) Brandbyge, M.; Mozos, J.-L.; Ordejon, O.; Taylor, J.; Stokbro, K. *Phys. Rev. B* **2002**, *65*, 165401.
(16) Larade, B.; Taylor, J.; Zheng, Q. R.; Mehrez, H.; Pomorski, P.; Guo, H. *Phys. Rev. B* **2001**, *64*, 195402.
(17) Soler, J. M.; Artacho, E.; Gale, J. D.; Garcia, A.; Junquera, J.; Ordejon, P.; Sanchez-Portal, D. *J. Phys.: Condens. Matter* **2002**, *14*, 2745.